PHYSICAL REVIEW B **66**, 060507(R) (2002)

Visualization of vortex chains in $Bi_2Sr_2CaCu_2O_{8+y}$ by magneto-optical imaging

M. Tokunaga,* M. Kobayashi, Y. Tokunaga, and T. Tamegai
Department of Applied Physics, The University of Tokyo, 7-3-1 Hongo, Bunkyo-ku, Tokyo 113-8656, Japan
(Received 4 May 2002; published 22 August 2002)

We visualized vortex chains in the crossing-lattices state in $Bi_2Sr_2CaCu_2O_{8+y}$ by using magneto-optical imaging technique. From the spacing of vortex chains, we could determine the anisotropy parameter quantitatively, from $\gamma=800\pm80$ for a slightly underdoped sample to $\gamma=490\pm50$ for slightly overdoped samples. Vortex chains can be rotated by changing the direction of in-plane field in the CuO_2 plane. Hysteretic motion and the forking of vortex chains are discussed in relation to the indirect pinning of Josephson vortices through pinning of pancake vortices.

DOI: 10.1103/PhysRevB.66.060507 PACS number(s): 74.60.Ec, 74.25.Dw, 74.25.Ha, 74.72.Hs

Recently, vortex states in highly anisotropic superconductors under tilted fields have attracted much interest.[1–13] In magnetic fields tilted from the c axis, characteristic arrangement of vortices in the ab plane of $Bi_2Sr_2CaCu_2O_{8+y}$ (BSCCO) was found by decoration measurements as early as 1991.[14] They clearly demonstrated the existence of a dense one-dimensional arrangement of vortices along the tilted direction (vortex chain) concomitantly with the usual vortex lattice. Judging from the evolution with tilting, the origin of vortex chains in BSCCO is considered to be different from that in moderately anisotropic $YBa_2(Cu_{1-x}Al_x)_3O_{7-\delta}$.[15–17] In the latter case, vortex chains are explained in the framework of anisotropic London model.[18–20] In highly anisotropic BSCCO, however, angular dependence of vortex-lattice melting field indicates that the scaling relation based on anisotropic Ginzburg-Landau model[21] is no longer available.[1,2] Both the existence of ''chain+lattice'' state and the new scaling were solved by considering the crossing-lattices state in which the pancake vortices (PV's) and Josephson vortices (JV's) coexist.[3] Such a coexistence of the orthogonal vortices was first proposed by Huse.[22] The most important point in Ref. 3 was the introduction of substantial attractive interactions between PV's and JV's caused by shifts of PV's by a current around a JV.

In the crossing-lattices state, two-component vortices attracting each other opened a new stage for vortex matter physics. Recent theoretical studies based on this model suggest the existence of various vortex phases in tilted fields.[7,11] Several experimental results of ac susceptibility,[4] transport,[5] and magnetization measurements,[6] indeed, manifest some features of transitions in vortex phases under tilted-fields close to the ab plane.

Attractive interactions between PV's and JV's enable us to control the arrangement of PV's by JV's. Recent direct observations by scanning Hall probe microscopy clearly demonstrate that one can manipulate PV's through the motion of JV's by changing the applied fields parallel to the ab plane.[8] Moreover, JV stacks play a role as a channel for penetration of PV's.[12] Such a controlled motion of PV's sheds a new light for possible applications of a PV stack as a ''bit'' in a logic device. Direct observations of vortices by Lorentz microscope[9] and magneto-optical imaging[12,13] also demonstrate some interesting nature of vortices in the crossing-lattices state. However, it is still an open question how much we can control JV's in this state, although it will be important for future applications.

We performed magneto-optical observations in BSCCO under crossing-lattices state. In our previous report,[12] we demonstrated the shift of a vortex puddle and creation of one-dimensional channels for vortex penetration caused by relatively high in-plane fields up to 3 kOe. In this paper, we focused on vortex distribution in the crossing-lattices state with low in-plane fields ($H_x \leqslant 110$ Oe). We observed vortex chains in the images, and studied the motion of the underlying JV stacks over the whole sample upon changing the magnitude and direction of in-plane fields. Observation of vortex chains enabled us to determine the anisotropy parameter $\gamma \equiv \sqrt{m_c/m_{ab}}$, where m_c and m_{ab} are the electronic mass along the c axis and ab plane, respectively.

BSCCO crystals were grown by the traveling solvent floating zone method. We controlled oxygen concentration by annealing under appropriate oxygen pressure. In this paper, we used slightly underdoped (no. 1), optimally doped (no. 2, no. 3), and slightly overdoped (no. 4) BSCCO crystals with the second magnetization peak at 27.5 K and critical temperature of $(H_p\ (\mathrm{Oe}), T_c\ (\mathrm{K}))=(230, 86)$, $(350, 91)$, $(350, 91)$, and $(380, 87)$, respectively. Magnetic induction perpendicular to the sample surface was visualized by magneto-optical imaging technique. Faraday rotation in a bismuth-doped garnet film mounted on the cleaved ab plane of the crystal was detected by a polarizing microscope and recorded by a cooled charge-coupled device camera.[12] To achieve a higher sensitivity, we utilized a differential method.[23] Namely, a difference between two images at different applied fields of $H_z+\delta H_z$ and $H_z-\delta H_z$, where z direction is parallel to the c axis, was stored and averaged over 50–1000 times. Due to this averaging process, it took about 8 min to 2 h to obtain one differential image in the present study. Magnetic fields parallel to the c axis (H_z) and ab plane (H_x) were applied independently with two sets of magnets. In this paper, we chose the y axis within the ab plane perpendicular to the H_x.

Figure 1 shows a differential image of sample no. 1 at $H_x=61$ Oe and $H_z=10\pm2.5$ Oe at 60 K. Direction of H_x is almost horizontal in Fig. 1 as shown by an arrow. We observed stripes with bright and dark contrast parallel to the H_x in the image. In this differential image, the brighter

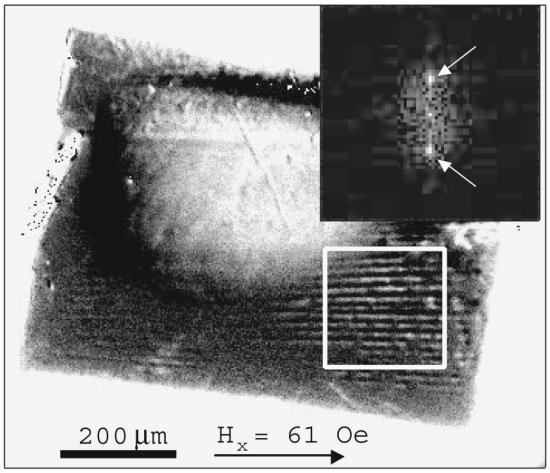

FIG. 1. Differential magneto-optical image on the ab plane of sample no. 1 for $H_z = 10 \pm 2.5$ Oe at 60 K. In-plane field of $H_x = 61$ Oe was applied parallel to the arrow. (Inset) Fast Fourier transformation of the image in the area marked by a white rectangle in the main panel.

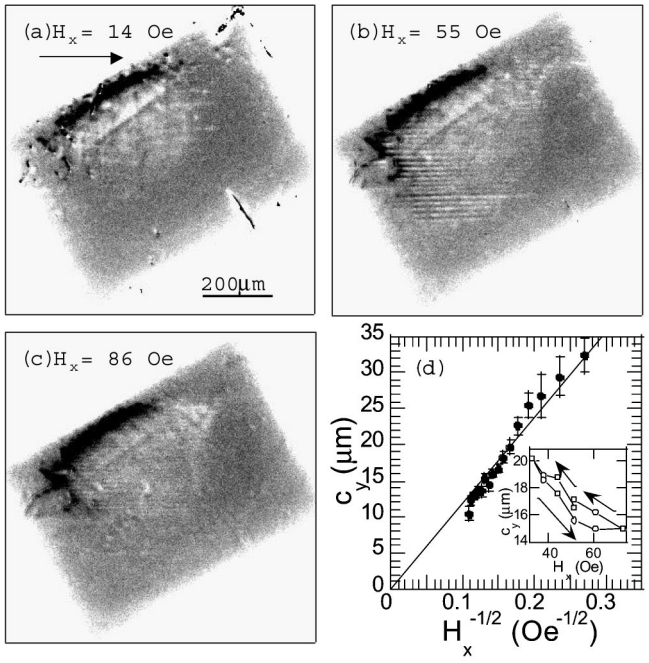

FIG. 2. Differential images at 60 K for $H_z = 10 \pm 1.5$ Oe and $H_x =$ (a) 14 Oe, (b) 55 Oe, and (c) 86 Oe. (d) H_x dependence of spacing of the stripes (c_y) at various area in the sample no. 1. Solid line indicates a fit by $c_y = \sqrt{\gamma \Phi_0 / \beta H_x}$, with $\gamma = 800$. Inset of (d) shows hysteresis in c_y against the cycle of the H_x ($H_x = 51 \rightarrow 32 \rightarrow 73 \rightarrow 51$ Oe).

(darker) regions correspond to the areas to which PV's penetrate more (less). The observed contrast on bright and dark lines corresponds to the difference of the change in magnetic induction (B) of about 200 mG. This magnitude is comparable to the average change of B over the entire sample, which is significantly reduced from the change of external fields ($2\delta H_z = 5$ Oe) due to the shielding effect. The period of stripes is well-defined. Actually, fast Fourier transformation (FFT) of the area marked by a white rectangle results in sharp peaks at finite k_y as pointed by arrows in the inset. Thus the defined period of stripes along the y direction (c_y) is about 20 μm at this condition. As will be shown later in detail, a rotation of H_x within the ab plane causes a rotation of stripes. This fact indicates that the stripes do not originate from any correlated pinning inherent to the sample but are generated by the in-plane field H_x.

Structure of the stripes is sensitive to the change of H_x. Figures 2(a–c) demonstrate evolution of the stripes upon increasing the value of H_x. At $H_x = 14$ Oe [Fig 2(a)], several bright lines almost parallel to the H_x are discernible near the center of the sample, and they are slightly modulated. As the H_x increases more, these stripes become more straight, and the spacing becomes smaller [$H_x = 55$ Oe in Fig. 2(b)]. The area in which stripes were observed changed between Fig. 1 and 2(b). This fact indicates that the region in which the chains are observed is not determined by any intrinsic nature in the sample, but depends on experimental setting. Contrast of the stripes becomes weaker by further increasing H_x up to 86 Oe due to the limited spatial resolution [Fig. 2(c)]. We could resolve each stripe up to about 110 Oe in our present system. Changing the average H_z from 7.5 to 15 Oe influences the contrast in differential images, while keeping the spacing of the stripes constant (not shown). The spacing is determined only by the in-plane component of the applied field. H_x dependence of the spacing of the stripes (c_y) is shown in Fig. 2(d). In this figure, we plot the average of c_y at various x coordinates. The error bar corresponds to the standard deviation. Although there is slight positional variation, overall profiles are roughly represented by a solid line of $c_y \propto H_x^{-1/2}$. This relation reminds us of the spacing of Josephson vortices $\sqrt{\gamma \Phi_0 / \beta H_x}$, where Φ_0 is the flux quantum, and β specifies arrangement of Josephson vortices.[24] With using $\beta = 2/\sqrt{3}$, the fitting gives $\gamma = 800 \pm 80$. This value is in reasonable agreement with that for underdoped BSCCO. Judging from the qualitative and quantitative agreement, we conclude that the observed stripes correspond to vortex chains located on the JV stacks. Since we applied relatively large H_z, the vortex state at these fields can hardly be the "chain" state but the "chain+lattice" state.[8] In the "chain+lattice" state, PV density within a chain increases faster than that in a lattice upon increase of H_z.[14] Thereby, we regard the observed each bright line as a vortex chain in the chain+lattice state.

In the crossing-lattices state, existence of vortex chains is based on the underlying JV's. We observed an irreversible motion of JV's upon changing H_x [inset of Fig. 2(d)]. The difference in c_y between increasing and decreasing processes of H_x amounts to 2 μm at $H_x = 51$ Oe even at the same area of the sample. Such an unusual counterclockwise hysteresis can be caused by the intrinsic pinning due to the layered structure.[25] Strong intrinsic pinning restricts the motion of JV's along the c axis. Hence, upon decreasing the H_x, JV's have to move more within the ab plane to achieve the equilibrium flux density. This process can be observed as the counterclockwise hysteresis of c_y.

With the temperature decreasing from 60 K, contrast in differential images becomes weaker corresponding to the in-

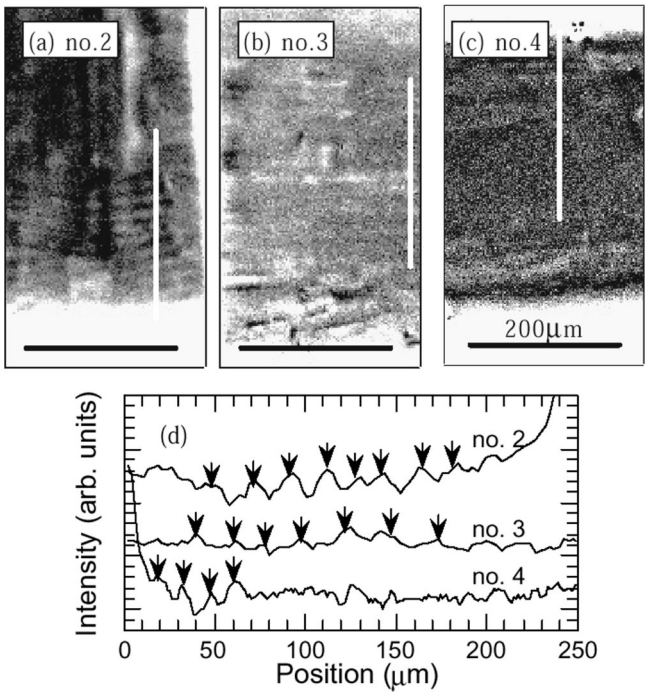

FIG. 3. Differential images for BSCCO with different oxygen concentrations, (a) optimally doped sample (no. 2) at $T=60$ K with $H_z=10\pm1.5$ Oe and $H_x=31$ Oe, (b) optimally doped sample (no. 3) at $T=65$ K with $H_z=8\pm2.5$ Oe and $H_x=32$ Oe, (c) slightly overdoped sample (no. 4) at $T=60$ K with $H_z=10\pm1.5$ Oe and $H_x=31$ Oe. (d) Line profiles along white lines in (a)–(c).

crease of pinning on PV's. Such a pinning impedes the motion of PV's, and hence reduces the difference between the two images at $H_z\pm\delta H_z$ in differential method. On the other hand, increase in temperature also diminishes contrast of stripes in differential images with $2\delta H_z=3$ Oe, possibly due to larger fluctuations on the vortex position. In the temperature range in which we resolved the chains (50 K$\leqslant T\leqslant$70 K), we did not observe any noticeable change of the chain spacing. Consequently, temperature dependence of γ should be small at least in this temperature range.

Next, let us move to the effect of oxygen concentration on the vortex chains. Figures 3(a–c) demonstrate the differential images for sample no. 2 to no. 4 at $H_x\sim30$ Oe. Doping of oxygen increases flux pinning on PV's, so that the contrast in the differential image becomes weaker as mentioned above. However, we can still identify the position of the chains in line-profiles of these images as shown by arrows in Fig. 3(d). Increase in oxygen concentration, i.e., doping level, is known to reduce γ.[26,27] In BSCCO, however, it has been difficult to determine the value of γ accurately from any experiment. By using $c_y=\sqrt{\gamma\Phi_0/\beta H_x}$, we determine the γ of sample no. 2, no. 3, and no. 4 as 590 ± 60, 650 ± 70, and 490 ± 50, respectively. This variation follows the tendency that the higher oxygen doping results in the smaller anisotropy.

In the following, we will show the motion of JV's with the rotation of H_x in sample no. 1. Figure 4(a) shows a differential image of sample no. 1 at 60 K after field cooling in $H_x=51$ Oe. Such a field cooling procedure results in straight chains parallel to the H_x direction as shown in Fig.

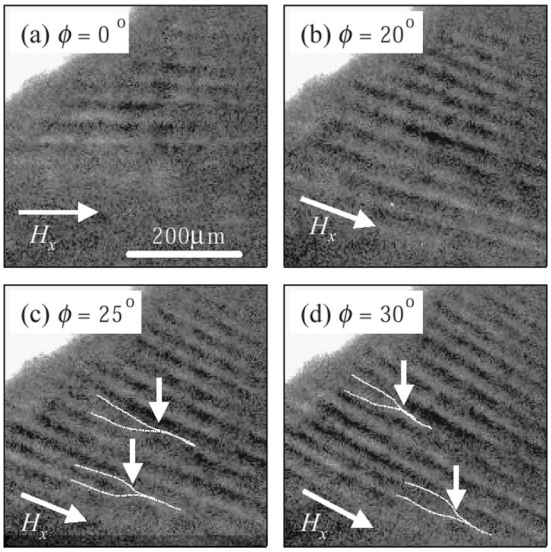

FIG. 4. Variation of the vortex chains by a rotation of H_x within the ab plane. (a) Stripe structure after field cooling at $H_x=51$ Oe ($\phi=0°$). Differential images were taken at $H_z=10\pm1.5$ Oe. Differential images after rotation of H_x to (b) $\phi=-20°$, (c) $\phi=-25°$, and (d) $\phi=-30°$. In Fig. 4(c), forking of a vortex chain takes place at the points marked by arrows. The points of forking move with further rotation of in-plane field in (d).

4(a). Hereafter, we set this direction as azimuthal angle $\phi=0°$. Upon rotating H_x within the ab plane to $\phi=-20°$, JV's and hence vortex chains follow the H_x direction [Fig. 4(b)]. On further rotation, we found the creation of a clear forking of vortex chains at the positions marked by arrows [Fig. 4(c)]. The points of forking move with further rotation to $\phi=-30°$. Such forking phenomena have been observed in other observations by changing the magnitude of H_x.[13] Since a single JV cannot terminate or split into two vortices, the forking can be ascribed to the splitting of JV stacks into different directions between different layers. The point here is that the forking can be generated by a rotation of H_x even without changing its magnitude. Thereby, we ascribed the origin not to the thermodynamic properties of the equilibrium state, but to irreversible nature caused by flux pinning.

Finally, we discuss the pinning effect on JV's in the crossing-lattices state. According to Ref. 3, crossing of a PV stack and a JV causes an energy gain (E_x) of

$$E_x=-\frac{2.1{\Phi_0}^2}{4\pi^2\gamma^2 s\ln(3.5\lambda_J/\lambda_{ab})}, \tag{1}$$

where λ_{ab} is the penetration depth within the ab plane and $\lambda_J=\gamma s$ represents the size of a JV core along the y direction. Number of the intersections is $1/c_z$ per unit length along the c axis, where $c_z=\sqrt{\beta\Phi_0/\gamma B_x}$ is a spacing of JV's along the c axis. The attractive force between a PV stack and a JV stack per unit length along the c axis is given by.

$$f_x=-\frac{E_x}{c_z\lambda_J}=\frac{1}{c_z\lambda_J}\frac{2.1{\Phi_0}^2}{4\pi^2\gamma^2 s\ln(3.5\lambda_J/\lambda_{ab})}. \tag{2}$$

With $\gamma=800$, $\lambda_{ab}=0.2$ μm, and $B_x=51$ G, we obtain $f_x=2.7\times10^{-5}$ dyn/cm. Smooth manipulation of PV's by a JV stack is possible if the pinning on PV's is smaller than this attractive force. The pinning force on the unit length of a PV stack can be estimated from the critical current density j_c as $f_p=(1/c)j_c\cdot\Phi_0$, where c is the speed of light. From magnetization measurements, we estimated the critical current density of sample no. 1 to $j_c=1.0$, 2.3, and 4.0×10^3 A/cm^2, and evaluated the pinning force to $f_p=2.1$, 4.8, and 8.3×10^{-5} dyn/cm at 70, 60, and 50 K, respectively. At lower temperatures, random point pinning on PV's dominates over the attraction by a JV stack. In practice, the pinning force does not act uniformly over the whole PV stack. When some PV's are fixed by the point pinning, some JV's will give up to hold the intersection, and hence, JV's stack may split out. The split JV's will attract other PV's around them. This scenario is conceivable to form an additional branch of vortex chain.

In conclusion, we observed vortex chains in $Bi_2Sr_2CaCu_2O_{8+y}$ under tilted fields by means of differential magneto-optical imaging. Observations of vortex chains enabled us to directly determine the anisotropy parameter for samples with various doping levels. The visualized characteristic motions of the underlying Josephson vortices upon the change in magnitude and direction of in-plane fields are discussed in relation to the effect of indirect pinning on Josephson vortices in the crossing-lattices state.

This work was supported by a Grant-in-Aid for Scientific Research from the Ministry of Education, Culture, Sports, Science and Technology.

*Electronic address: mtokunaga@ap.t.u-tokyo.ac.jp URL: http://moo.t.u-tokyo.ac.jp/mtokunaga/

[1] B. Schmidt *et al.*, Phys. Rev. B **55**, R8705 (1997).
[2] S. Ooi *et al.*, Phys. Rev. Lett. **82**, 4308 (1999).
[3] A.E. Koshelev, Phys. Rev. Lett. **83**, 187 (1999).
[4] M. Konczykowski *et al.*, Physica C **341-348**, 1213 (2000).
[5] J. Mirković *et al.*, Phys. Rev. Lett. **86**, 886 (2001).
[6] S. Ooi *et al.*, Phys. Rev. B **63**, 020501 (2001).
[7] S.E. Savel'ev, J. Mirković, and K. Kadowaki, Phys. Rev. B **64**, 094521 (2001).
[8] A.N. Grigorenko *et al.*, Nature (London) **414**, 728 (2001).
[9] T. Matsuda *et al.*, Science **294**, 2134 (2001).
[10] A Buzdin and I. Baladié, Phys. Rev. Lett. **88**, 147002 (2002).
[11] M.J.W. Dodgson, Phys. Rev. B **66**, 014509 (2002).
[12] M. Yasugaki *et al.*, Phys. Rev. B **65**, 212502 (2002).
[13] V.K. Vlasko-Vlasov *et al.*, Phys. Rev. B **66**, 014523 (2002).
[14] C.A. Bolle *et al.*, Phys. Rev. Lett. **66**, 112 (1991).
[15] P.L. Gammel *et al.*, Phys. Rev. Lett. **68**, 3343 (1992).
[16] I.V. Grigorieva, J.W. Steeds, and K. Sasaki, Phys. Rev. B **48**, 16 865 (1993).
[17] I.V. Grigorieva *et al.*, Phys. Rev. B **51**, 3765 (1995).
[18] A.M. Grishin, A.Y. Martynovich, and S.V. Yampolsky, Zh. Éksp. Teor. Fiz. **97**, 1930 (1990) [Sov. Phys. JETP **70**, 1089 (1990)].
[19] A.I. Buzdin and A.Yu. Simonov, Zh. Éksp. Teor. Fiz. **98**, 2074 (1990) [Sov. Phys. JETP **71**, 1165 (1990)].
[20] L.L. Daemen, L.J. Campbell, and V.G. Koyan Phys. Rev. B **46**, 3631 (1992).
[21] G. Blatter, V.B. Geshkenbein, and A.I. Larkin, Phys. Rev. Lett. **68**, 875 (1992).
[22] D.A. Huse, Phys. Rev. B **46**, 8621 (1992).
[23] A. Soibel *et al.*, Nature (London) **406**, 282 (2000).
[24] L.J. Campbell, M.M. Doria, and V.G. Kogan, Phys. Rev. B **38**, 2439 (1988).
[25] M. Tachiki and S. Takahashi, Solid State Commun. **70**, 291 (1989).
[26] T. Yasuda, S. Takano, and L. Rinderer, Physica C **208**, 385 (1993).
[27] Y. Kotaka *et al.*, Physica C **235-240**, 1529 (1994).